이학석사 학위 논문

Effect of subdiaphragmatic vagotomy on acute inflammatory pain

급성 통증에 대한 횡경막 아래 미주신경절단술의 효과

2022년 2월

서울대학교 대학원
자연과학대학 뇌인지과학과 전공
김 예 진

Effect of subdiaphragmatic vagotomy on acute inflammatory pain

Advisor: Prof. Seog Bae Oh, D.D.S, Ph.D.

Submitting a master's thesis of
Nature Sciences

February 2022

Graduate School of Natural Sciences
Seoul National University
Brain and Cognitive Sciences Major

Yea Jin Kim

Confirming the master's thesis written by
Yea Jin Kim
February 2022

Chair	이인아	(Seal)
Vice Chair	오석배	(Seal)
Examiner	우충완	(Seal)

ABSTRACT

Effect of subdiaphragmatic vagotomy on acute inflammatory pain

Yea Jin Kim

Brain and Cognitive Sciences Major

Graduate School of Natural Science

Seoul National University

Subdiaphragmatic vagotomy (SDV) produces analgesic effect in various pain conditions including not only visceral pain but also somatic pain. I aimed to determine how SDV induces analgesic effect in somatic pain condition by using formalin-induced acute inflammatory pain model. I analyzed c-Fos expression in the whole brain and identified specific brain region mediating SDV-induced analgesic effect on acute inflammatory pain. I found that c-Fos expression was specifically increased in the anterior insular cortex (aIC) among subregions of the insular cortex in acute inflammatory pain, which was reversed by SDV. These results were not mimicked in female mice, indicating sexual-dimorphism in SDV-induced analgesia. SDV decreased c-Fos expressions more preferentially in glutamatergic neurons rather than GABAergic neurons in the aIC, and pharmacological activation of glutamatergic neurons with NMDA (1 μg/μL) in the aIC inhibited SDV-induced analgesic effect. Taken together, this study suggests that the decrease in the neuronal activity of glutamatergic neurons in the aIC mediates SDV-induced analgesic effect, potentially serving as an important therapeutic target to treat inflammatory pain.

Keyword: Subdiaphragmatic vagotomy (SDV); acute inflammatory pain; anterior insular cortex; glutamatergic neuron

Student Number: 2020-27479

CONTENTS

LIST OF FIGURES

ABBREVIATIONS

ACC	Anterior cingulate cortex
aIC	Anterior insular cortex
BLA	Basolateral amygdala
CeA	Central amygdala
IC	Insular cortex
LH	Lateral hypothalamus
lPBN	Lateral parabrachial nucleus
mIC	Medial insular cortex
mPFC	Medial prefrontal cortex
NAcC	Nucleus accumbens core
NAcS	Nucleus accumbens shell
NMDA	N-methyl-D-aspartate
NTS	Nucleus tractus solitaries
pIC	Posterior insular cortex
RVM	Rostralventromedial medulla
SDV	Subdiaphragmatic vagotomy
vlPAG	ventrolateral periaqueductal gray
VMH	ventromedial hypothalamus

INTRODUCTION

1.1. Study Background

Pain is one of the most prevalent symptom in various disease and a common health problem worldwide.[19, 41] Pain is mainly treated with medications, which are sometimes combined with therapies to change lifestyles especially for the management of chronic pain patients.[15, 46] When medications are proven to be ineffective for pain patients, several surgical interventions may help to control pain in certain pain conditions.[50] Interestingly, it has been reported that vagotomy relieves pain in some patients and subdiaphragmatic vagotomy (SDV) attenuates pain under pathological conditions in the adult rodents.[1, 13, 42, 43, 59]

SDV is a surgery to dissect the bilateral vagus nerve that is responsible for the bidirectional communication nerve relaying information between the gut and the brain.[10] Clinical studies have demonstrated that SDV reduces gastric acid of the stomach and attenuates pain in patients with a stomach ulcer or upper gastrointestinal neoplasms.[1, 43] Also, a preclinical study showed that SDV partially suppresses visceral pain induced by a functional dyspepsia model.[13] While the effect of SDV has been well studied with focus on visceral disease and is critically associated with visceral pain,[13, 49, 59] recent studies have demonstrated that SDV can relieve somatic pain as well.[27, 43] I also confirmed SDV-induced analgesia in formalin-induced acute inflammatory pain condition.[27, 34] Given SDV attenuates pain originated from extraterritorial area which is not innervated by vagus nerve, supraspinal mechanisms are highly likely to contribute to SDV-induced analgesia in somatic pain conditions.

SDV commonly accompanies the changes in the brain because vagus nerve mainly relays visceral information from the gastrointestinal tract to the brain.[10] Indeed, SDV produces changes of brain derived neurotrophic factor and corticotropin-releasing hormone in the brain region associated with pain under visceral pain condition.[13] Moreover, SDV reduces pro-inflammatory gene

expression in brain regions such as the basolateral amygdala (BLA) and central amygdala (CeA) in LPS-induced inflammatory pain condition.[44] I also observed that SDV produces pain reduction only in the second phase, not first phase, of formalin test under acute inflammatory pain condition.[27, 34] As the second phase of formalin test is known to be mediated by central mechanisms,[16, 52] brain mechanisms might be also involved in SDV-induced analgesia. However, it is not fully understood how the brain mechanisms underlie SDV-induced analgesia in somatic pain conditions.

Insula cortex (IC) is a crucial region mainly recognizing the information arising from the stomach.[35] Therefore, SDV blocks the activation of the IC induced by lithium chloride injection which causes visceral stimuli.[49] In addition, the IC is closely involved in pain perception,[11] and especially the anterior insular cortex (aIC), a subarea of the IC, is highly implicated in inflammatory pain.[5] I also showed that c-Fos expression is significantly enhanced in the aIC by formalin-induced somatic acute inflammatory pain.[31] Furthermore, the glutamatergic signaling in the IC plays a crucial role in modulating pain perception.[57] Given these observations, I hypothesized that the glutamatergic neurons in the aIC may contribute to SDV-induced analgesic effect in the acute inflammatory pain condition.

In the current study, I thus focused on the involvement of the aIC on SDV-induced analgesic effect, by employing the behavior test, immunohistochemical analysis, and pharmacological manipulations. Here, I elucidate the involvement of glutamatergic neurons in the aIC for SDV-induced analgesia in acute inflammatory pain, which may provide a potential brain therapeutic target for the treatment of inflammatory pain.

1.2. Purpose of Research

Although it is well known that the subdiaphragmatic vagotomy (SDV) induces analgesic effects on acute inflammatory pain, it remains elusive how SDV induces analgesia. Here, I have explored the brain mechanism that may mediate SDV-induced analgesia by examining pattern of c-Fos expression, identifying change in glutamatergic or GABAergic neurons of the aIC and then confirmed

their involvement with pharmacological manipulation.

- To elucidate brain mechanism responsible for SDV-induced analgesic effect on acute inflammatory pain.

MATERIALS AND METHOD

Animals

Both Male and female C57BL/6 mice and female weighing 20-25g (5 to 8-week-old) were used for the experiment and purchased from DooYeol Biotech (South Korea). All animals were maintained (5 per cage) at a temperature-controlled room (23 ± 1℃), and a 12-12h light/dark cycle with standard lab chow (pellet diet) and water *ad libitum*. All experimental procedures were reviewed and approved by Institutional Animal Care and Use Committee (IACUC) at Seoul National University (protocol code: SNU-200604-2-5). All experiments were performed in accordance with relevant guidelines and regulations that were confirmed by IACUC.

Bilateral subdiaphragmatic vagotomy (SDV)

The procedure of bilateral subdiaphragmatic vagotomy was performed as follows. The mice were anesthetized by intraperitoneal injection of pentobarbital (50mg/kg, *i.p.*). Following anesthetization, the mice were placed in the supine position under a microscope. An incision of 3 cm long in the abdomen was made through skin and muscle. The liver was gently displaced to expose the esophagus. The vagus nerve (anterior and posterior) was removed using the surgical scissor and forceps just below the diaphragm. Next, the abdominal muscles and the skin were sutured with surgical sutures. For sham surgery, the branches of the vagus nerve were gently exposed but not cut. After surgery, the mice were placed in their cage and were recovered for one week. After all of the experiments were finished, I verified the success of SDV by observing increase in the stomach size **(Fig. 1E)**.[40]

Formalin test

Before the behavior test, mice were placed in a white acrylic chamber before experiment for two hours for three consecutive days to allow them to adapt to their surroundings. To observe the hind paw, a mirror was placed at a 45° angle

below the chamber.

I used the formalin-induced acute inflammatory pain model as previously described.[33] 20 μL of 1% formalin (formaldehyde solution, 36~38%, Junsei, Japan) was injected subcutaneously into the plantar surface of the left hind paw with a 0.3 mL insulin syringe. After formalin injection, the mice were immediately placed in the test chamber and recorded using a video camera for 40 minutes. The time of licking and flinching was measured during each 5minutes.

Administration of drugs

N-methyl-D-aspartate (NMDA, N-methyl-D-aspartate receptor agonist; M2004, MO, USA) was purchased from Sigma-Aldrich. For activation of the aIC, NMDA (0.2 or 1 μg/μL) was diluted in 0.9% normal saline. The concentration and time of NMDA for activation were determined according to previous investigations using dose with 0.1, 0.5, 1.0 μg/side.[3, 39, 53] However, since I confirmed through pilot study that mice were died within 10 minutes after systemic administration of 1.0 μg/side, I did use lower than 2.0 μg/μL.

Stereotaxic surgeries

To activate glutamatergic neurons with NMDA in the aIC, C57BL/6 mice were anesthetized by pentobarbital (50 mg/kg, *i.p.*) and implanted with a guide cannula (26-gauge, 3.0 mm of length, Plastics One) and secured by dental acrylic in the aIC (coordinates: anteroposterior (AP) +2.5 from, mediolateral (ML) +2.5 from the midline, dorsoventral (DV) -3.2 from skull surface). Following a week recovery period, mice were operated sham or SDV surgery. After sham or SDV surgery, mice were allowed to recover for one week before the behavioral test was performed. When inserted for drug injection in the aIC, microinjector tips extended 0.2 mm beyond the guide. The volume of NMDA for the single-site was 0.5 μL. The rate of injection was 0.2 μL/min with 10 minutes for diffusion. After 10 minutes from drug injection, 20 μL of 1% formalin was injected in left hind paw.

After the formalin tests were concluded, mice were perfused with phosphate-

buffered saline (0.1 M PBS; pH 7.4) and 4% paraformaldehyde (PFA), and the brains were harvested for histologic identification of specific protein and confirmation of correct injection placement in the aIC.

Immunohistochemistry

To identify c-Fos expression using DAB immunohistochemistry after anesthetization with the administration of pentobarbital (50 mg/kg, *i.p.*) 1 hours after formalin injection, mice were perfused with PBS and 4% PFA for immunohistochemistry of c-Fos proteins. The brains were post-fixed 4℃ by 4% PFA overnight after extraction and cryoprotected in 30% sucrose solution for three days. Brains were frozen and cut at -22℃ in a section of 40 μm. The tissues were preserved in PBS and incubated with hydrogen peroxide (H_2O_2) for 30 minutes to prevent endogenous peroxide activity at room temperature (RT) and then washed three times in 0.1M PBS. The tissues were blocked for 1 hour with 5% normal goat serum diluted with 0.3% Triton X-100 in PBS (0.3% PBST) at RT and incubated in rabbit c-Fos antibody (1:1000 dilution, ab190289, Abcam, Cambridge, UK) diluted in 0.3% PBST, 1% normal goat serum for 2 days at 4℃. Following incubation in the primary antibody, the tissues were washed several times for 10 minutes in 0.1 M PBS and incubated for 2 hours in biotinylated goat anti-rabbit (1:200 dilution, BA-1000, Vector Laboratories, CA, USA) in 0.1M PBS at RT. After 2 hours, the sections were processed with ABC kit (VECTASTAIN ABC kit, PK-6100, Vector laboratories, CA, USA) for 1 hour at RT. To visualize immunoreactivity, the sections were incubated with DAB kit (DAB substrate kit for peroxidase, SK-4100, Vector laboratories, CA, USA) and washed several times in 0.1 M PBS. Then, the sections were mounted on coated glass slides. Following air drying, all tissues were dehydrated through a series of graded ethanol from 80% ethanol to pure ethanol and clearing agents. All tissues were covered with permountant (Sigma-Aldrich, MO, USA).

To detect NeuN and c-Fos expression, sections were incubated for 1 hour in blocking buffer (0.3% Triton X-100, 5% normal donkey serum in 0.1 M PBS) at room temperature. The primary antibodies are chicken anti-NeuN (1:400 dilution, ABN78, Millipore, MA, USA) and rabbit anti-c-Fos (1:400 dilution,

ab190289, Abcam, Cambridge, UK) were diluted in the blocking solution, and the sections were incubated for one day at 4℃. The sections were washed several times for 10 minutes each in 0.1 M PBS. The secondary antibodies A488 donkey anti-chicken (1:400 dilution, 703-545-155, Jackson, PA, USA), Cy3 donkey anti-rabbit (1:400 dilution, 711-165-152, Jackson, PA, USA), and DAPI (1:1000 dilution, D9545, Sigma Aldrich, MO, USA) were diluted in 0.1 M PBS and incubated 1 hour at RT. The slices were then washed several times for 10 minutes with 0.1 M PBS and mounted using VECTASHIELD mounting media (Vector Laboratories, CA, USA).

To visualize CaMKII expression, brain sections were incubated for 1 hour in blocking solution (0.3% Triton X-100, 2% bovine serum in 0.1 M PBS) at room temperature. The primary antibodies mouse anti-CaMKII (1:200 dilution, MA1-048, Thermofisher, MA, USA) and rabbit anti-c-Fos (1:400 dilution, ab190289, Abcam, Cambridge, UK) were diluted in the blocking solution, and the sections were incubated for 48 hours at 4℃. The sections were three times for 10 minutes each in 0.1 M PBS. The sections were incubated for 2 hours in biotinylated goat anti-mouse (BP-9200, Vector laboratories, CA, USA) at RT. After 2 hours, the sections were washed three times for 10 minutes with 0.1 M PBS. Then, the sections were processed with the secondary antibodies Streptavidin+Cy3 (1:200 dilution, SA-1300, Vector Laboratories, CA, USA), Alexa 488 goat anti-rabbit (1:300 dilution, 111-545-003, Jackson, PA, USA), and DAPI (1:1000 dilution, D9542, Sigma Aldrich, MO, USA) in 0.1 M PBS for 2 hours at RT. The sections were then washed three times for 10 minutes with 0.1 M PBS and mounted using VECTASHIELD mounting media (Vector Laboratories, CA, USA).

To identify GAD67 expression for counting, brains were cut in a section of 20 μm. The tissues were incubated for an hour in blocking solution (0.3% Triton X-100, 8% normal donkey serum in 0.1 M PBS) at RT. The primary antibodies mouse anti-GAD67 (1:400 dilution, ab26116, Abcam, Cambridge, UK) and rabbit anti-c-Fos (1:400 dilution, ab190289, Abcam, Cambridge, UK) were diluted in the blocking solution for 24 hours at RT. After treatment of primary antibodies, the tissues were washed three times for 10 minutes with 0.1 M PBS. The secondary antibodies FITC donkey anti-rabbit (1:400 dilution,

711-095-152, Jackson, PA, USA), Cy3 donkey anti-mouse (1:400 dilution, 715-165-150, Jackson, PA, USA), and DAPI (1:1000 dilution, D9542, Sigma Aldrich, MO, USA) were diluted in 0.1 M PBS and incubated for an hour. The tissues were washed several times for 10 minutes with 0.1 M PBS and mounted using VECTASHIELD mounting media (Vector Laboratories, CA, USA). To visualize GAD67 expression for representative images, the sections were incubated for an hour in blocking solution (0.3% Triton X-100, 5% bovine serum, 5% normal goat serum in 0.1 M PBS) at room temperature. The primary antibodies mouse anti-GAD67 (1:500 dilution, MAB5406, Sigma-Aldrich, MO, USA) and rabbit anti-c-Fos (1:500 dilution, ab190289, Abcam, Cambridge, UK) were diluted in the blocking solution for 2 days overnight at 4℃. After 2 days, the sections were washed three times for 10 minutes with 0.1 M PBS. The secondary antibodies Cy3 goat anti-mouse (1:500 dilution, 115-165-206, Jackson, PA, USA), Alexa 488 goat anti-rabbit (1:500 dilution, 111-545-003, Jackson, PA, USA), and DAPI (1:1000 dilution, D9542, Sigma Aldrich, MO, USA) were diluted in 0.1 M PBS and incubated for 2 hours at RT. The sections were then washed several times with 0.1 M PBS and mounted using VECTASHIELD mounting media (Vector Laboratories, CA, USA).

Image analysis

Mounted slides were examined under the bright-field microscope (DM5000B, Leica, Germany). All images were taken at 10× magnification with identical lighting intensity and color balance conditions. To analyze c-Fos expression within the brain region of interest, I collected 4 to 6 sections per mouse (n=4-5 each group). All visible c-Fos-IR-positive neurons were counted, and the mean value was used as representative counts. Using Image J software (National Institutes of Health), the images were converted to greyscale, background subtracted, sharped and enhanced contrast, and intensity threshold were adjusted. Expression of c-Fos protein was analyzed for the following regions: the distance from the bregma in the rostrocaudal plane is from +1.98 to 1.6 mm for the anterior insular cortex (aIC) and medial prefrontal cortex (mPFC), +0.61 mm for medial insular cortex (mIC), from +1.4 to 1.0 mm for the anterior cingulate cortex (ACC), nucleus accumbens core (NAcC) and shell (NAcS),

from -0.11 mm to -0.23 mm for posterior insular cortex (pIC), -1.22 mm for the basolateral amygdala (BLA), central amygdala (CeA), lateral hypothalamus (LH) and ventromedial hypothalamus (VMH), -5.02 mm for the ventrolateral periaqueductal gray (vlPAG), lateral parabrachial nucleus (lPBN) and the rostral ventromedial medulla (RVM), and -6.96 mm for the nucleus tractus solitaries (NTS). The locations of the brain regions were previously described.[32]

All immunofluorescent-stained sections were imaged on a confocal microscope (LSM 700, Carl Zeiss, Germany). I collected six sections per mouse (n=5 mice each group), and all images were taken at 200× or 400× magnification. Image analysis was performed manually by identifying and counting $CaMKII^{+}$ and $GAD67^{+}$ in the same area.

Statistical analysis

Statistical analysis was performed using GraphPad Prism version 8.0 (GraphPad Software, CA, USA). Comparison between two groups was made using the unpaired Student's t-test. For multiple comparisons, data were analyzed using the one-way or two-way ANOVA followed by the post hoc Bonferroni test. Detailed statistics for each experiment were shown in the figure legend. Data are presented as mean ± SEM. Differences with $p < 0.05$ were considered significant.

RESULTS

The verification of subdiaphragmatic vagotomy (SDV)

To validate whether subdiaphragmatic vagotomy (SDV) surgery is completely administrated, I operated on surgery as a representative schedule and surgery scheme **(Figs. 1A, 1B)**. The anterior and posterior vagus nerve locations before SDV surgery are depicted **(Figs. 1C, 1D)**. One week after SDV surgery, I observed that the dilatation of the stomach in the SDV-operated group was more extensive than those in the sham-operated group **(Fig. 1E)**.

SDV suppressed nociceptive behavior in formalin-induced acute inflammatory pain

I first confirmed whether SDV indeed produces the analgesic effect on nociceptive behaviors in the acute inflammatory pain condition. I used formalin model, which is widely used to study acute inflammatory pain in many animal models.[2, 33, 34] A formalin test was performed one week after SDV or sham surgery in the male adult mice **(Fig. 2A)**. Consistent with previous studies including our recent work,[27, 34] I observed that SDV significantly suppressed nociceptive behavior during the second phase, not the first phase, of the formalin test **(Figs. 2B, 2C)**.

SDV reversed enhancement of c-Fos expression in the aIC produced by formalin injection

To map SDV-induced brain activity pattern using c-Fos as an direct marker of neuronal activity as described in the previous study, I checked the patterns of c-Fos expression in whole brain regions related to homeostasis and pain modulation under acute inflammatory pain conditions.[30, 32] I monitored the immunoreactivity (IR) of c-Fos in the whole brain regions of the sham and formalin-treated sham group. Consistently with a previous study, I observed that formalin injection significantly increased the number of c-Fos immunoreactive cells in the anterior insular cortex (aIC) and other brain regions **(Fig. 3A)**.

To investigate brain regions mediating SDV-induced analgesic effect under acute inflammatory pain conditions, I compared the patterns of c-Fos expression in the whole brain regions of formalin-treated sham and SDV groups. Among the groups, I observed a profound change of c-Fos density in the contralateral aIC, ACC and mPFC between formalin-treated sham and SDV group **(Fig. 3A)**.

Furthermore, since the involvement of the aIC in analgesic effect induced the reduction of neural activation,[25] I focused on the aIC.

The aIC only showed change of c-Fos expression pattern among subregions of the insular cortex

There are three subregions in the insular cortex (IC) along the rostro-caudal axis that is divided into the anterior, medial and posterior insular cortex.[18] The subregions of the IC are closely associated with pain perception because the aIC is mainly involved in the affective-motivational aspect and the posterior insular cortex (pIC) mainly mediates the sensory-discriminative aspect of pain.[7, 14] To investigate which subregion of the IC is specifically involved in SDV-induced analgesic effect under acute inflammatory pain condition, I examined immunoreactivity (IR) of c-Fos expression in subregions (i.e. aIC, mIC and pIC) of the IC between the formalin-treated sham and SDV groups. The number of c-Fos expression was significantly reduced in the aIC of the formalin-treated SDV group compared to the sham group **(Fig. 4B)**. In contrast, the number of c-Fos expression in the mIC and pIC showed no significant change between the formalin-treated sham and SDV groups **(Figs. 4D, 4F)**. Taken together, these results demonstrated the potential role of the aIC in SDV-induced analgesic effect.

SDV-induced analgesic effect was specific to male mice

I next asked whether SDV induced analgesic effect is sex-specific and repeated behavior tests in the female mice under formalin-induced acute inflammatory pain condition **(Fig. 5A)**. Unlike male mice, the results showed that the nociceptive behavior did not change with SDV in female mice **(Figs. 5B, 5C)**. I also analyzed c-Fos expression in the female group to determine brain regions which showed changes of neuronal activation following SDV in male mice. In contrast to result in male mice, the number of c-Fos expression in the aIC was similar between formalin-treated sham and SDV groups **(Fig. 5E)**. I also observed a dramatic increase in the ACC and mPFC of the formalin-treated SDV group compared to the sham group **(Figs. 5G, 5I)**. Overall, these results indicated that sex difference exists in SDV-induced analgesic effect under acute inflammatory pain condition.

SDV decreased activation of glutamatergic neurons in the aIC under acute inflammatory pain condition

It has been demonstrated that insular cortex contains 73% of glutamatergic neurons and 27% of GABAergic neurons.[26] I thus explored whether the effect of SDV induces changes of activity in glutamatergic or GABAergic neuron within the aIC by double immunostaining with their specific markers and c-Fos expression. Glutamatergic and GABAergic neurons were confirmed with fluorescent immunostaining of calcium calmodulin kinase II (CaMKII) and glutamic acid decarboxylase 67 (GAD67), respectively **(Fig. 6A)**.[8, 36] As indicated by colocalization of c-Fos and CaMKII **(Figs 6B, 6C)**, the number of co-localized glutamatergic neurons was decreased in the aIC of formalin-treated SDV group. In contrast, the effect of SDV did not affect the number of c-Fos and GAD67 colocalization in the aIC of formalin-treated SDV group **(Figs. 6D, 6E)**. These results imply that reduced activity of glutamatergic neurons in the aIC contributes to SDV-induced analgesic effect.

NMDA microinjection into the aIC reversed SDV-induced analgesic effect in acute inflammatory pain

To verify involvement of glutamatergic neurons in the aIC in SDV-induced analgesic effect, I employed a pharmacological experiment with NMDA to activate glutamatergic neurons in the aIC. Mice were implanted by cannula in the aIC to administrate NMDA (0.2 or 1 μg/μL) or vehicle as shown in Fig. 7A. I examined the injection site by Evans blue into cannula at the end of experiments and excluded incorrect microinjector placement from data **(Fig. 7B)**. I observed that the number of c-Fos expression in the aIC increased with microinjection of NMDA **(Fig. 7C)**. The dose was determined based on previous studies and my pilot result.[3, 39, 53] Although the effect of NMDA was minimal with 0.2 μg/μL concentration, 1.0 μg/μL NMDA increased nociceptive behaviors in the second phase of formalin test **(Figs. 7D and 7E)**. These results indicated that activation of glutamatergic neurons in the aIC reverses SDV-induced analgesic effect.

Figure 1.

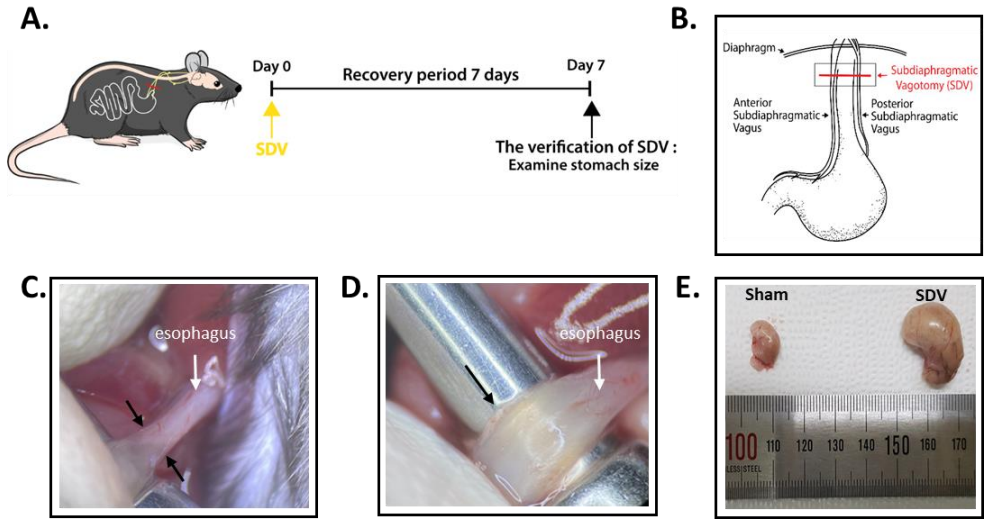
A.
Day 0
Recovery period 7 days
Day 7
SDV
The verification of SDV :
Examine stomach size
B.
Diaphragm
Subdiaphragmatic
Vagotomy (SDV)
Anterior
Subdiaphragmatic
Vagus
Posterior
Subdiaphragmatic
Vagus
C.
esophagus
D.
esophagus
E.
Sham
SDV
100
110
120
130
140
150
160
170

Figure 1. The verification of subdiaphragmatic vagotomy (SDV)

(A) Schedule and **(B)** schematic diagram of the SDV surgery. The visual operative field for SDV surgeries. Microscopic photography of **(C)** the anterior vagus nerve (black arrowheads) and **(D)** the posterior vagus nerve (black arrowhead) at esophagus level (white arrowheads). **(E)** Representative photograph of the stomach size after sham or SDV surgery.

Figure 2.

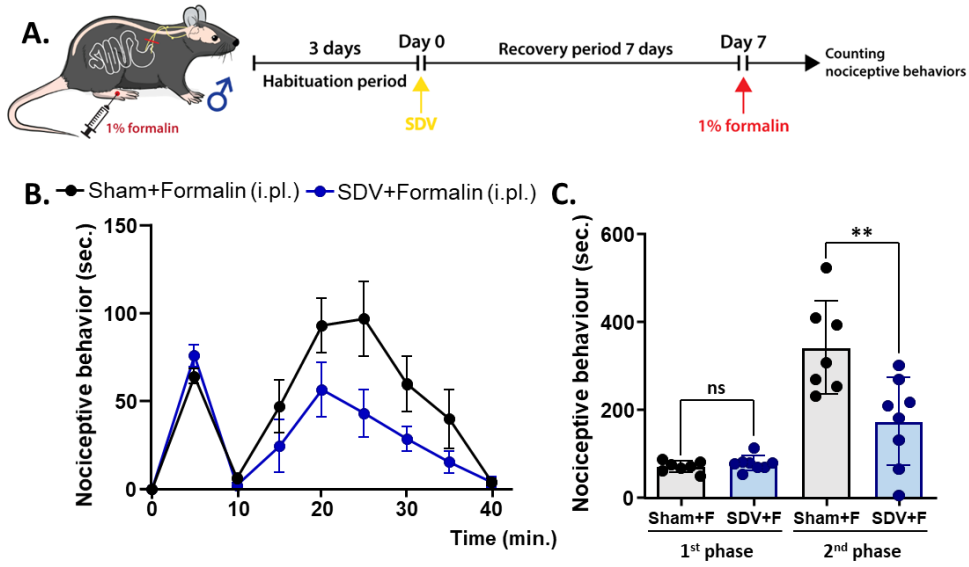
A.
1% formalin
3 days
Habituation period
Day 0
SDV
Recovery period 7 days
Day 7
1% formalin
Counting
nociceptive behaviors
B.
Sham+Formalin (i.pl.)
SDV+Formalin (i.pl.)
Nociceptive behavior (sec.)
150
100
50
0
0
10
20
30
40
Time (min.)
C.
Nociceptive behaviour (sec.)
600
400
200
0
ns
**
Sham+F
SDV+F
Sham+F
SDV+F
1st phase
2nd phase

Figure 2. Effect of SDV in formalin-induced acute inflammatory pain

(A) Schematic diagram of experiment schedule design. **(B)** Effect of SDV on formalin-induced acute inflammatory pain in male mice (n=7 and 8 for sham and SDV, respectively). **(C)** Comparison for nociceptive behavior in the first and second phase of formalin test between formalin-treated sham and formalin-treated SDV groups. Data are presented as mean ± SEM. ***p* <0.01 (unpaired Student's t-test).

Figure 3.

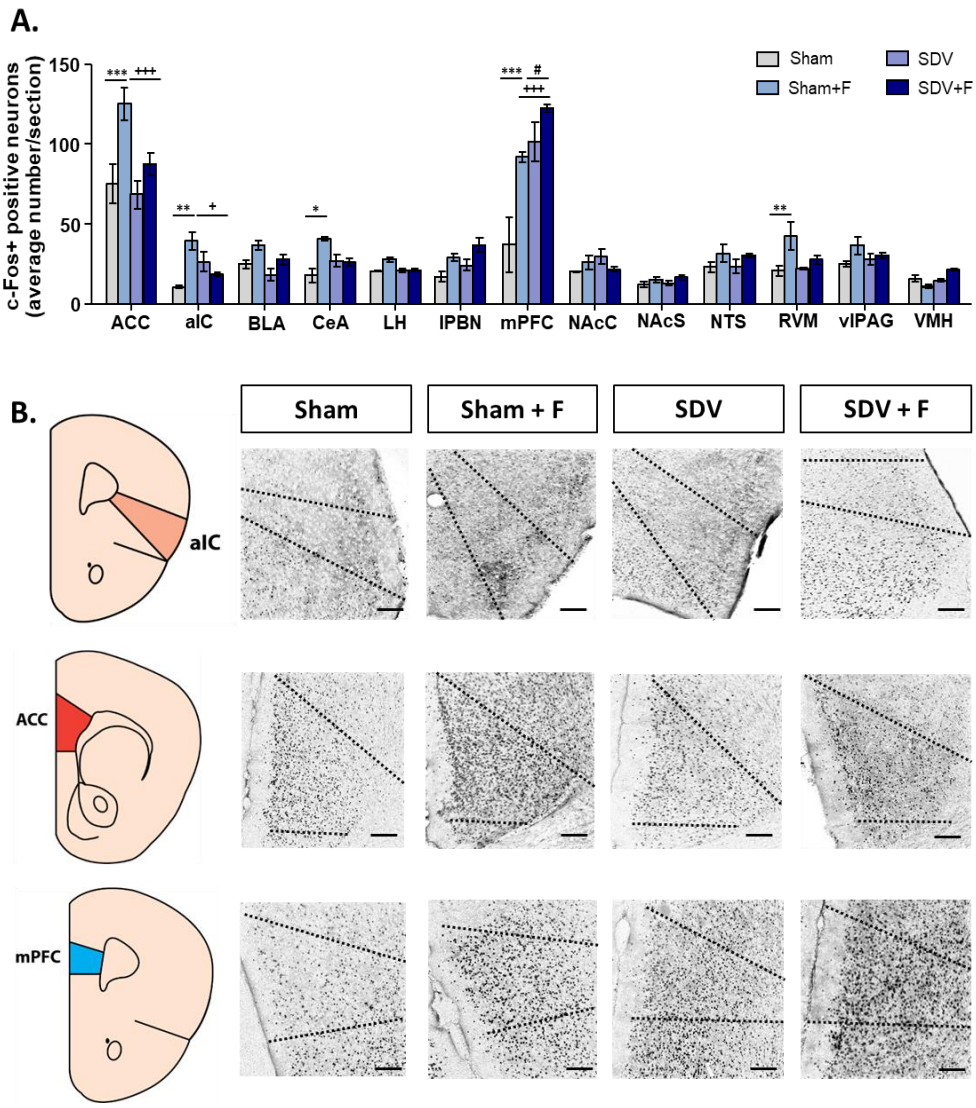
A.
c-Fos+ positive neurons (average number/section)
150
100
50
0
Sham
Sham+F
SDV
SDV+F
***
+++
**
+
*
***
#
+++
**
ACC
aIC
BLA
CeA
LH
lPBN
mPFC
NAcC
NAcS
NTS
RVM
vlPAG
VMH
B.
Sham
Sham + F
SDV
SDV + F
aIC
ACC
mPFC

Figure 3. The patterns of c-Fos expression in the whole brain regions associated with homeostasis and pain modulation in formalin-treated SDV group

(A) Average number c-Fos+ cell count in different group of sham, formalin-treated sham, SDV, and formalin-treated SDV groups on acute inflammatory pain. **(B)** Schematic representation and representative photomicrographs of c-Fos observed in the aIC, ACC and mPFC. Scale bar represents 100 μm; magnification 10×. Representative regions in coronal sections based on the atlas of Paxinos and Watson (2nd edition). Asterisk represents significant changes of c-Fos between sham and formalin-treated sham groups. Cross represents significant changes of c-Fos between formalin-treated sham and formalin-treated SDV group. Sharp represents significant changes of c-Fos between SDV and formalin-treated SDV group. Data are presented as mean ± SEM. *p <0.05, **p <0.01, ***p <0.001; +p <0.05, ++p <0.01, +++p <0.001; #p <0.05, ##p <0.01, ###p <0.001 (two-way ANOVA followed by Bonferroni test).

Figure 4.

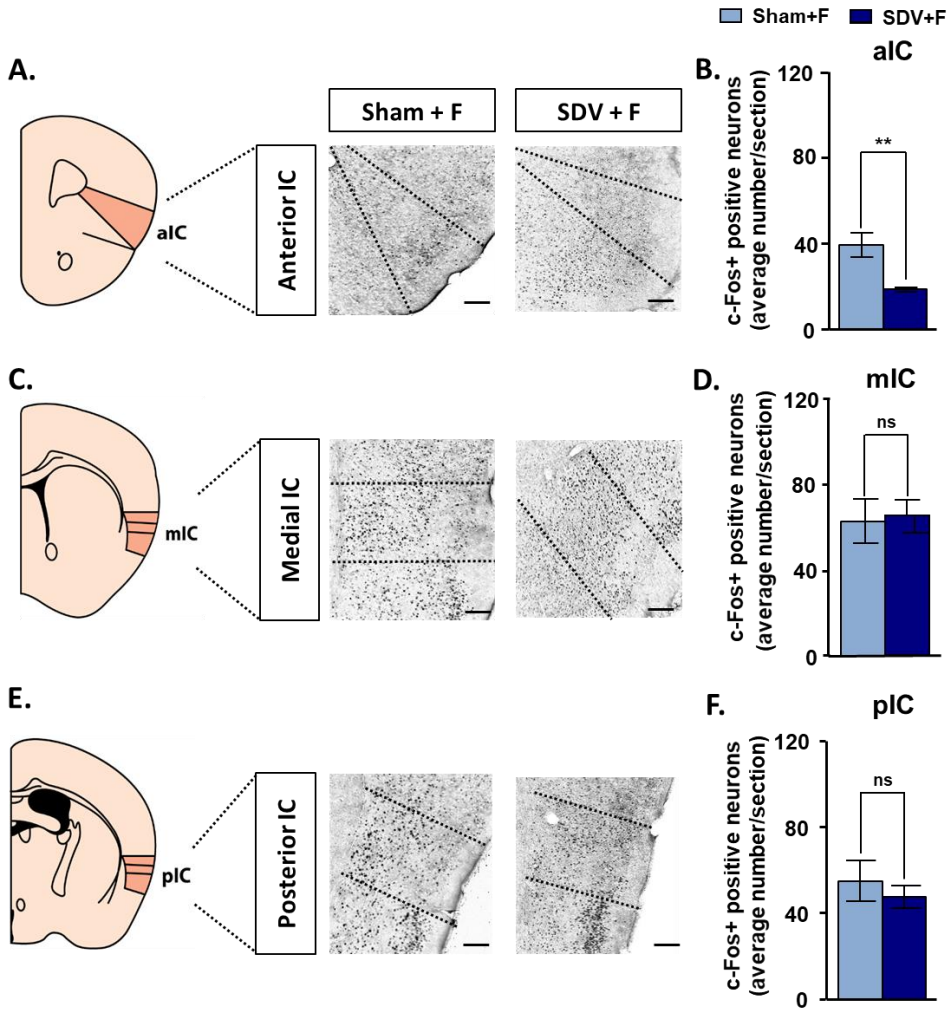
A.
Sham + F
SDV + F
aIC
Anterior IC
B.
Sham+F
SDV+F
aIC
c-Fos+ positive neurons (average number/section)
120
80
40
0
**
C.
mIC
Medial IC
D.
mIC
ns
E.
pIC
Posterior IC
F.
pIC
ns

Figure 4. The patterns of c-Fos expression in the subregions of the insular cortex in formalin-treated SDV group

(A) Schematic representation and representative photomicrographs of c-Fos observed in the aIC of formalin-treated sham and formalin-treated SDV groups. **(B)** Average number c-Fos+ cell count in the aIC of formalin-treated sham and formalin-treated SDV groups on acute inflammatory pain. **(C)** Schematic representation and representative photomicrographs of c-Fos observed in the medial IC (mIC) of formalin-treated sham and formalin-treated SDV groups. **(D)** Average number c-Fos+ cell count in the mIC of formalin-treated sham and formalin-treated SDV groups on acute inflammatory pain. **(E)** Schematic representation and representative photomicrographs of c-Fos observed in the posterior IC (pIC) of formalin-treated sham and formalin-treated SDV groups. **(F)** Average number c-Fos+ cell count in the pIC of formalin-treated sham and formalin-treated SDV groups on acute inflammatory pain. Representative regions in coronal sections based on the atlas of Paxinos and Watson (2nd edition). Scale bar represents 100 μm; magnification 10× Data are presented as mean ± SEM. ***p* <0.01 (unpaired Student's t-test).

Figure 5.

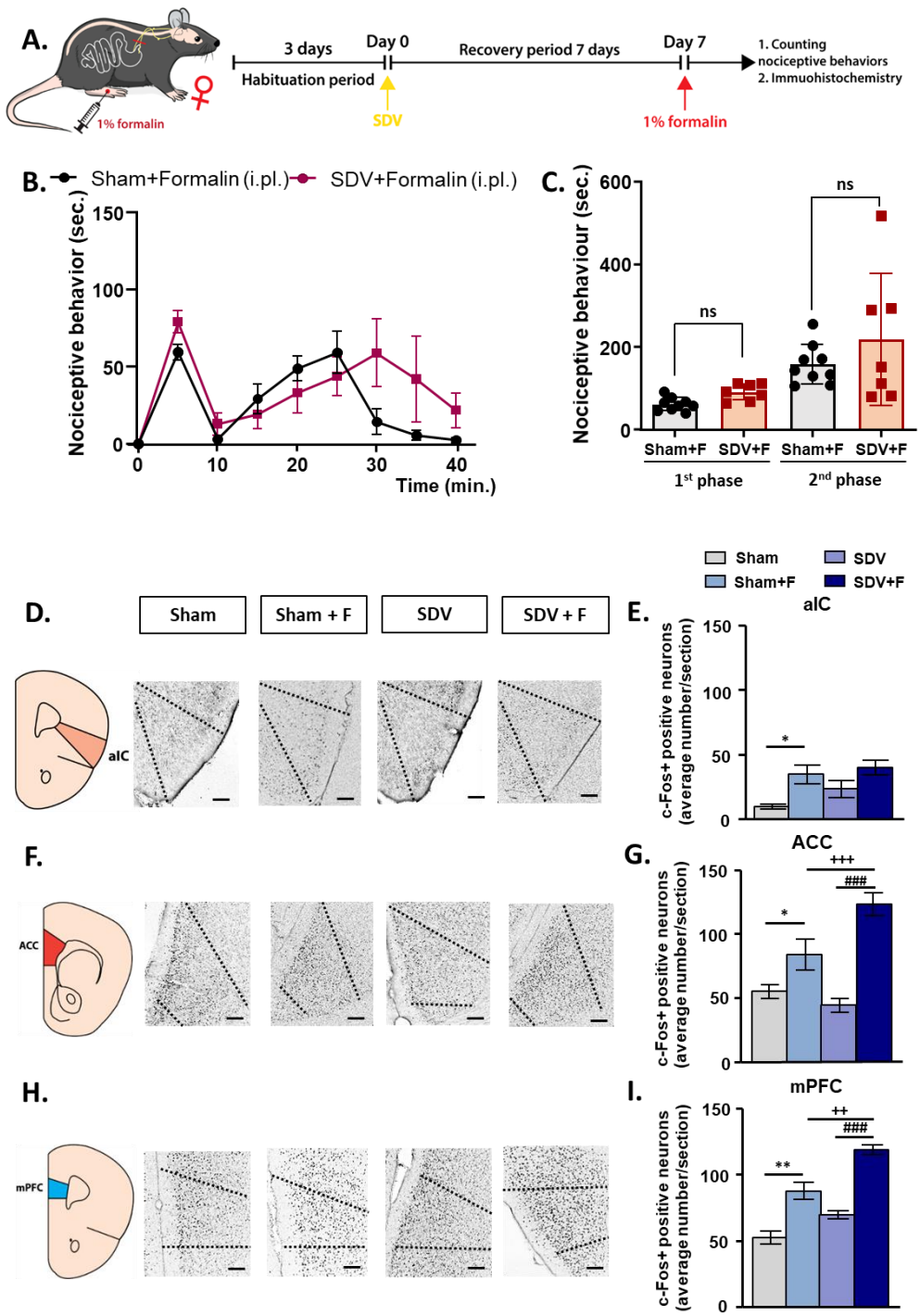
A.
1% formalin
3 days
Habituation period
Day 0
SDV
Recovery period 7 days
Day 7
1% formalin
1. Counting nociceptive behaviors
2. Immuohistochemistry
B.
Sham+Formalin (i.pl.)
SDV+Formalin (i.pl.)
Nociceptive behavior (sec.)
Time (min.)
C.
Nociceptive behaviour (sec.)
ns
Sham+F
SDV+F
1st phase
2nd phase
D.
Sham
Sham + F
SDV
SDV + F
aIC
E.
Sham
Sham+F
SDV
SDV+F
aIC
c-Fos+ positive neurons (average number/section)
F.
ACC
G.
ACC
H.
mPFC
I.
mPFC

Figure 5. The patterns of c-Fos expression in the aIC, ACC and mPFC in formalin-treated SDV group in female mice

(A) Schematic diagram of experiment schedule design. **(B)** No effect of SDV on formalin-induced acute inflammatory pain in female mice (n=9 and 7 for sham and SDV, respectively). **(C)** Comparison for nociceptive behavior in the first and second phase of formalin test between formalin-treated sham and formalin-treated SDV groups in female mice. **(D)** Schematic representation of the aIC and representative photomicrographs of c-Fos observed in the aIC of female mice. **(E)** Average number c-Fos+ cell count in the aIC of all groups on acute inflammatory pain. **(F)** Schematic representation of the ACC and representative photomicrographs of c-Fos observed in the ACC of female mice. **(G)** Average number c-Fos+ cell count in the ACC of all groups on acute inflammatory pain. **(H)** Schematic representation of the mPFC and representative photomicrographs of c-Fos observed in the mPFC of female mice. **(I)** Average number c-Fos+ cell count in the mPFC of all groups on acute inflammatory pain. Scale bar represents 100 μm; magnification 10×. Asterisk represents significant changes of c-Fos between sham and formalin-treated sham groups. Cross represents significant changes of c-Fos between formalin-treated sham and formalin-treated SDV groups. Sharp represents significant changes of c-Fos between SDV and formalin-treated SDV groups. Data are presented as mean ± SEM. *p <0.05, **p <0.01, ***p <0.001; +p <0.05, ++p <0.01, +++p <0.001; #p <0.05, ##p <0.01, ###p <0.001 (two-way ANOVA followed by Bonferroni test).

Figure 6.

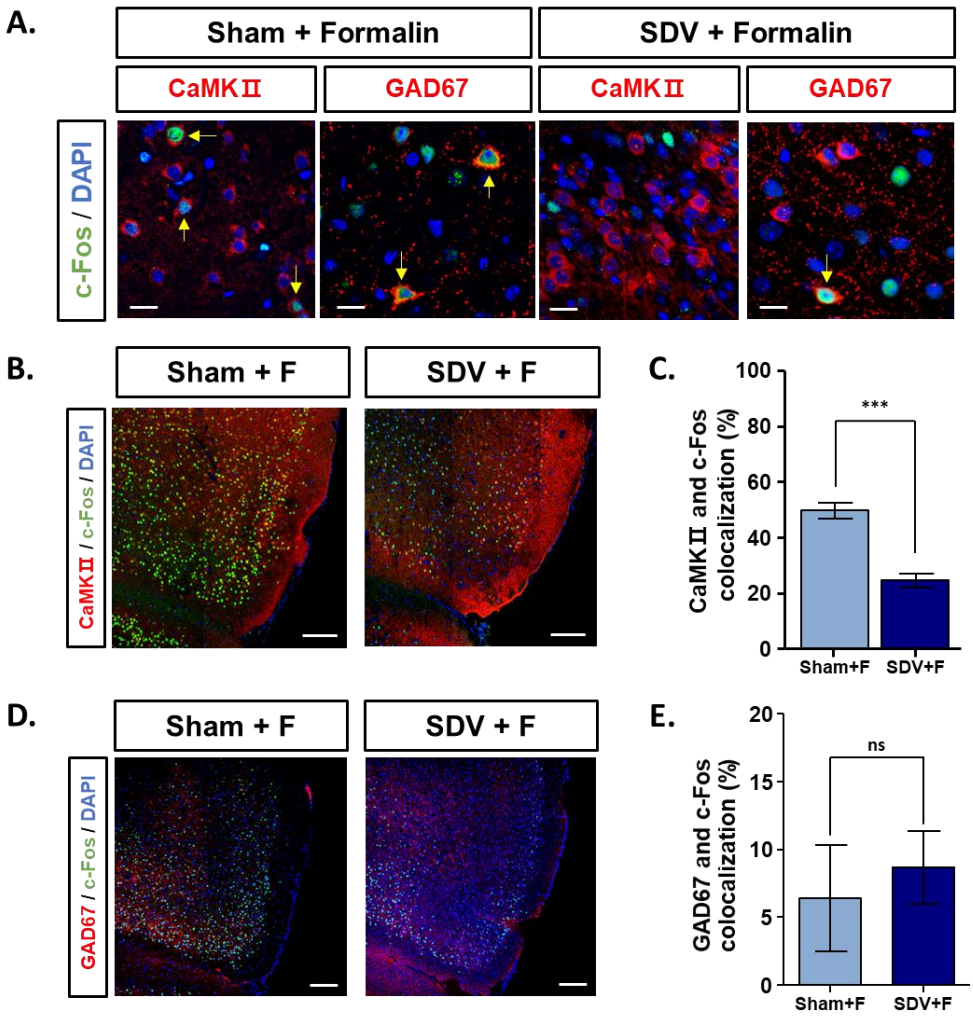
A.
Sham + Formalin
SDV + Formalin
CaMKⅡ
GAD67
CaMKⅡ
GAD67
c-Fos / DAPI
B.
Sham + F
SDV + F
CaMKⅡ / c-Fos / DAPI
C.
CaMKⅡ and c-Fos colocalization (%)
100
80
60
40
20
0
***
Sham+F
SDV+F
D.
Sham + F
SDV + F
GAD67 / c-Fos / DAPI
E.
GAD67 and c-Fos colocalization (%)
20
15
10
5
0
ns
Sham+F
SDV+F

Figure 6. The expression of CaMKII and GAD67 colocalization with c-Fos-positive neurons in the aIC

(A) Representative fluorescence image illustrating expression of CaMKII or GAD67 (red), c-Fos (green), and DAPI (blue) in the aIC of formalin-treated sham and formalin-treated SDV groups. Scale bar represents 20 μm; magnification 400×. **(B)** Representative fluorescence image illustrating expression of CaMKII (red, yellow arrow indicates co-labeled neurons), c-Fos (green), and DAPI (blue) in the whole aIC of formalin-treated sham and formalin-treated SDV groups. Scale bar represents 10 μm; magnification 200×. **(C)** Comparison for levels of CaMKII and c-Fos colocalization in the aIC of formalin-treated sham and formalin-treated SDV groups. **(D)** Representative fluorescence image illustrating expression of GAD67 (red, yellow arrow indicates co-labeled neurons), c-Fos (green), and DAPI (blue) in the whole aIC of formalin-treated sham and formalin-treated SDV groups. Scale bar represents 10 μm; magnification 200×. **(E)** Comparison for levels of GAD67 and c-Fos colocalization in the aIC of formalin-treated sham and formalin-treated SDV groups. Data are presented as mean ± SEM. ***p <0.001 (unpaired Student's t-test).

Figure 7.

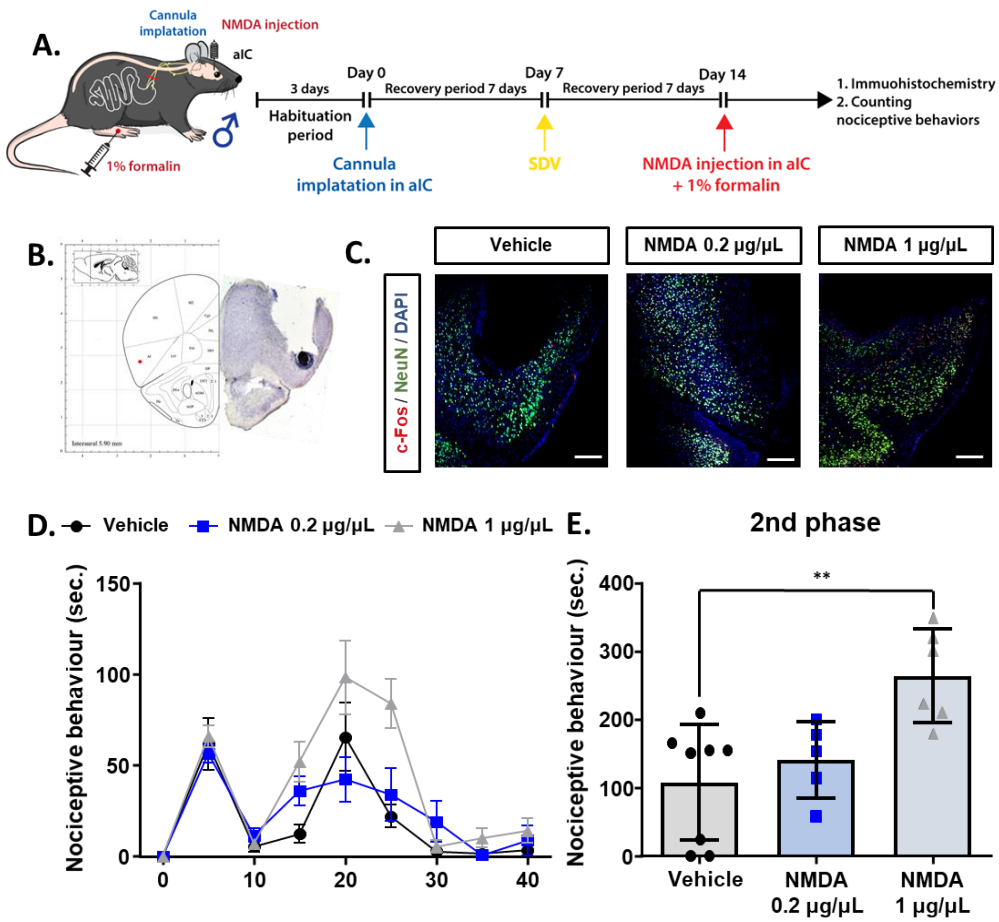
A.
Cannula implatation
NMDA injection
aIC
1% formalin
3 days
Habituation period
Day 0
Recovery period 7 days
Day 7
Recovery period 7 days
Day 14
1. Immuohistochemistry
2. Counting nociceptive behaviors
Cannula implatation in aIC
SDV
NMDA injection in aIC + 1% formalin
B.
C.
Vehicle
NMDA 0.2 μg/μL
NMDA 1 μg/μL
c-Fos / NeuN / DAPI
D.
Vehicle
NMDA 0.2 μg/μL
NMDA 1 μg/μL
Nociceptive behaviour (sec.)
150
100
50
0
0
10
20
30
40
E.
2nd phase
Nociceptive behaviour (sec.)
400
300
200
100
0
**
Vehicle
NMDA 0.2 μg/μL
NMDA 1 μg/μL

Figure 7. Effect of activation of glutamatergic neurons in the aIC on SDV-induced analgesia

(A) Schematic diagram of experiment schedule design. **(B)** Location of microinjection site in the aIC with atlas of Paxinos and Watson (2nd edition). **(C)** Representative fluorescence image illustrating expression of c-Fos (red), NeuN (green), and DAPI (blue) in the aIC of formalin-treated SDV group after vehicle or NMDA microinjection. Scale bar represents 10 μm; magnification 200×. **(D)** Change in nociceptive behavior of formalin-treated SDV group with NMDA or vehicle infusion (n=5-8 per group) **(E)** Comparison for nociceptive behavior in the formalin-treated SDV group with NMDA or vehicle injection in the second phase of formalin test. Data are presented as mean ± SEM. ***p* <0.05 (one-way ANOVA followed by Bonferroni test).

Figure 8.

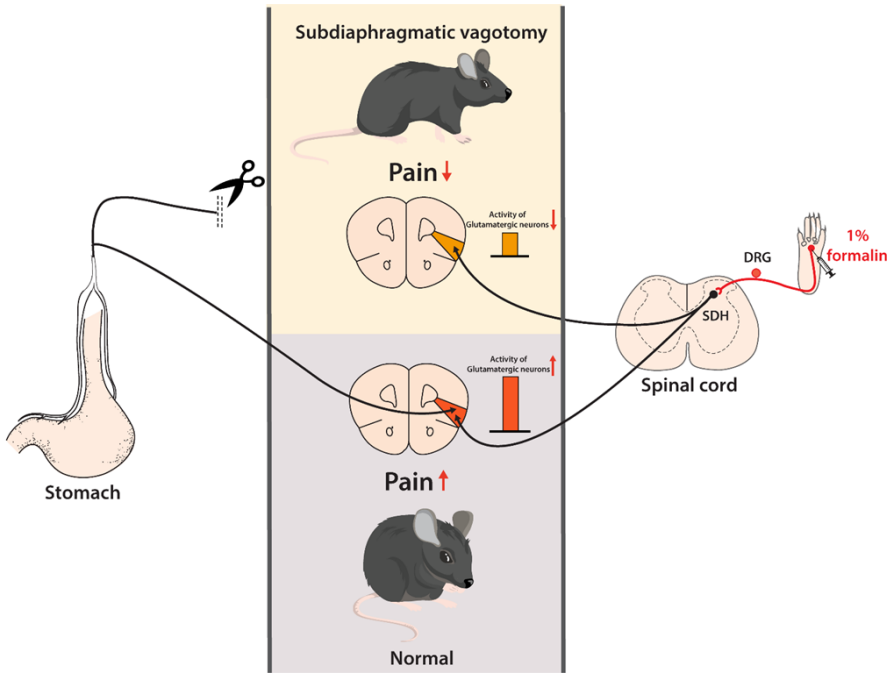
Subdiaphragmatic vagotomy
Pain
Activity of Glutamatergic neurons
DRG
1% formalin
SDH
Spinal cord
Stomach
Activity of Glutamatergic neurons
Pain
Normal

Figure 8. Schematic summary showing that activity of glutamatergic neuron in the aIC plays a key role in SDV-induced analgesia under acute inflammatory pain condition

DISCUSSION

In this study, I demonstrated critical involvement of the aIC in SDV-induced analgesia in acute inflammatory pain. I further confirmed that decrease in neuronal activities of glutamatergic neurons in the aIC which are enhanced under acute inflammatory pain condition contributes to SDV-induced analgesia **(Fig. 8)**. Thus, my work delineates a brain mechanism responsible for SDV-induced analgesic effect.

My results indicate that decrease in neuronal activities of the aIC which are enhanced under acute inflammatory pain condition contributes to SDV-induced analgesia. A previous report also strongly support the notion that analgesic effect is closely linked to the reduction in neural activation of IC.[25] A clinical research that investigating how nutrient signals are transmitted from the gastrointestinal tract to the brain, shows that the brain regions connected to the gastrointestinal tract are also involved in modulating pain.[55] In the previous study, the activities of these brain regions were decreased by vagotomy. It suggests that the analgesic effect can be induced by reducing the brain region's activity as the signals from the gastrointestinal tract were reduced following vagotomy. In particular, the anterior insular cortex (aIC) is a critical brain region modulating the sense of the internal state in the body, such as interoception, and receiving the signal from the stomach.[35, 56] It can be inferred that the activity of the aIC is decreased by vagotomy, and this reduced activity affects pain modulation. However, further study is needed to clarify whether the reduced activity of the aIC is involved in the decrease of signals from the gastrointestinal tract.

Prominent change of c-Fos expression was only observed in the aIC among the subregions of the IC **(Figs. 3A, 4B)**, while there was no difference in the number of c-Fos expression within the IC between formalin-treated sham and SDV groups (data not shown). The subregions of the IC play different roles in pain perception[37] because the aIC is mainly involved in the affective-motivational pain and the posterior insular cortex (pIC) preferably participates

in the sensory-discriminative pain.[7, 14] Because SDV decreased c-Fos expression only in aIC, but not in other subregions of the IC, it seems SDV might regulate affective-motivational components rather than sensory-discriminative components in pain. In line with this, it has been reported that SDV induces a decreased inner anxiety behavior[28] and depression-like behavior.[48] Thus, it can be inferred association between improvement of negative emotion caused by SDV[13, 28, 48] and involvement of aIC in the affective pain.[24]

The IC is activated during acute and chronic pain in human[4] and rodent.[6, 9, 38] Since glutamatergic neuron accounts for a major subtype of neurons in the IC,[26] elevated glutamate within the IC has used the markers for the presence of central sensitization or pain centralization.[17, 21-23] Additionally, the pain produces increase of the excitatory synaptic transmission in the aIC.[5] Therefore, it can be suggested that glutamatergic neuron in the aIC is activated by noxious stimuli, and modulation of glutamatergic neuron in the aIC is a favored strategy for regulating pain.[58] As examples related to this suggestion, the reduced glutamatergic signaling within the IC decreases nociceptive pain behavior in chronic pain[57] and specifically chemogenetic inhibition of glutamatergic neuron in the aIC produced analgesic effect in pain condition.[5] In consistency with the previous studies, I also observed that SDV caused reduced activity of glutamatergic neurons in the aIC **(Fig. 6C)**, and activation of glutamatergic neuron in the aIC induced pain via pharmacological manipulation with NMDA **(Figs. 7D, 7E)**. Therefore, it can be inferred that glutamatergic neuron in the aIC may be clinical potential target to regulate pain. However, limitation of my study is that I did not use chemogenetics tool to activate specifically glutamatergic neuron in the aIC. Nevertheless, combined with behavior test, immnuohistochemical staining and pharmacological manipulations, my current data can suggest that SDV-induced analgesic effect is involved in glutamatergic neuron within the aIC.

As a result of analyzing exactly SDV-induced analgesia via the pattern of c-Fos expression without biased view, I checked a profound change of neuronal activity in the ACC and mPFC **(Fig. 3A)**. I observed the decreased expression in the ACC and increased expression in the mPFC in the formalin-treated SDV group compared to the formalin-treated sham group. The pattern of neuronal

activity in the ACC is comparable to that of the aIC **(Fig. 3A)**. The connectivity between the ACC and aIC is well known as pain modulation, especially in affective-dimension pain.[11, 20] The previous study has shown that the involvement of the ACC in analgesic effect induced the reduction of neuronal activity.[54] It suggests that the ACC can be another target mediating SDV-induced analgesic effect under acute inflammatory pain condition. Additionally, SDV induces the change of limbic neurotransmitters, such as dopamine in the mPFC related to pain modulation.[29, 45] The neuronal activity of the mPFC, projected from the dopaminergic neurons in the ventral tegmental area (VTA), is increased by activation of dopaminergic neuron.[12] Therefore, consistently with my result **(Fig. 3A)**, it can be inferred that the increase of dopamine following SDV induces neuronal activation in the mPFC.

I observed that SDV did not significantly suppress the second phase of the formalin test in female mice **(Figs. 5B, 5C)**. In the previous study, while SDV and gonadectomy suppressed the nociceptive behavior in the second phase, the estrogen increased nociceptive behavior.[27] Moreover, unlike male mice, I showed different patterns of c-Fos expression in the aIC of female mice **(Fig. 5E)**. Previous research has examined that the significant activation of the insular cortex is induced by intravenous (*i.v.*) injection of estrogen.[51] Therefore, I can assume that the SDV-induced analgesia was not observed in female mice due to activation of the IC caused by a gonadal hormone, such as estrogen.

SDV entails structural and functional changes in the brain, including the nucleus of the solitary tract (NTS).[29, 47, 55] A previous study has demonstrated that total anterograde tracer arising from the left cervical vagus to the NTS was decreased until 10 days of SDV, whereas the number of tracer was similar to that of control group at 30 days following SDV.[47] Therefore, I designed all experiments to be completed within 10 days following SDV when the effect of SDV could be most clearly observed and verified the success of SDV surgery via excessive stomach expansion in SDV-operated mice **(Figs. 1E, 2A)**.[40]

In conclusion, this study indicates that subdiaphragmatic vagotomy (SDV) suppresses nociceptive behavior via reduction of glutamatergic neuron activity in the anterior insular cortex under formalin-induced acute inflammatory pain condition **(Fig. 8)**. Therefore, these results suggest that the aIC provide a new

alternative for therapeutic target to modulate acute inflammatory pain.

REFERENCE

1. Ajao OG. Vagotomy for relief of pain in some upper gastrointestinal neoplasms. *J Natl Med Assoc.* 69:655-658, 1977

2. Alhadeff AL, Su Z, Hernandez E, Klima ML, Phillips SZ, Holland RA, Guo C, Hantman AW, De Jonghe BC, Betley JN. A Neural Circuit for the Suppression of Pain by a Competing Need State. *Cell.* 173:140-152 e115, 2018

3. Alijanpour S, Zarrindast MR. Potentiation of morphine-induced antinociception by harmaline: involvement of mu-opioid and ventral tegmental area NMDA receptors. *Psychopharmacology (Berl).* 237:557-570, 2020

4. Apkarian AV, Bushnell MC, Treede RD, Zubieta JK. Human brain mechanisms of pain perception and regulation in health and disease. *Eur J Pain.* 9:463-484, 2005

5. Bai Y, Ma LT, Chen YB, Ren D, Chen YB, Li YQ, Sun HK, Qiu XT, Zhang T, Zhang MM, Yi XN, Chen T, Li H, Fan BY, Li YQ. Anterior insular cortex mediates hyperalgesia induced by chronic pancreatitis in rats. *Mol Brain.* 12:76, 2019

6. Becerra L, Chang PC, Bishop J, Borsook D. CNS activation maps in awake rats exposed to thermal stimuli to the dorsum of the hindpaw. *Neuroimage.* 54:1355-1366, 2011

7. Benarroch EE. Insular cortex: Functional complexity and clinical correlations. *Neurology.* 93:932-938, 2019

8. Berg L, Eckardt J, Masseck OA. Enhanced activity of pyramidal neurons in the infralimbic cortex drives anxiety behavior. *PLoS One.* 14:e0210949, 2019

9. Borsook D, Becerra L. CNS animal fMRI in pain and analgesia. *Neurosci Biobehav Rev.* 35:1125-1143, 2011

10. Breit S, Kupferberg A, Rogler G, Hasler G. Vagus Nerve as Modulator of the Brain-Gut Axis in Psychiatric and Inflammatory Disorders. *Front*

Psychiatry. 9:44, 2018

11. Bushnell MC, Ceko M, Low LA. Cognitive and emotional control of pain and its disruption in chronic pain. *Nat Rev Neurosci.* 14:502-511, 2013

12. Chung AS, Miller SM, Sun Y, Xu X, Zweifel LS. Sexual congruency in the connectome and translatome of VTA dopamine neurons. *Sci Rep.* 7:11120, 2017

13. Cordner ZA, Li Q, Liu L, Tamashiro KL, Bhargava A, Moran TH, Pasricha PJ. Vagal gut-brain signaling mediates amygdaloid plasticity, affect, and pain in a functional dyspepsia model. *JCI Insight.* 6, 2021

14. Craig AD. How do you feel? Interoception: the sense of the physiological condition of the body. *Nat Rev Neurosci.* 3:655-666, 2002

15. De Gregori M, Muscoli C, Schatman ME, Stallone T, Intelligente F, Rondanelli M, Franceschi F, Arranz LI, Lorente-Cebrian S, Salamone M, Ilari S, Belfer I, Allegri M. Combining pain therapy with lifestyle: the role of personalized nutrition and nutritional supplements according to the SIMPAR Feed Your Destiny approach. *J Pain Res.* 9:1179-1189, 2016

16. Dubuisson D, Dennis SG. The formalin test: a quantitative study of the analgesic effects of morphine, meperidine, and brain stem stimulation in rats and cats. *Pain.* 4:161-174, 1977

17. Foerster BR, Petrou M, Edden RA, Sundgren PC, Schmidt-Wilcke T, Lowe SE, Harte SE, Clauw DJ, Harris RE. Reduced insular gamma-aminobutyric acid in fibromyalgia. *Arthritis Rheum.* 64:579-583, 2012

18. Gehrlach DA, Weiand C, Gaitanos TN, Cho E, Klein AS, Hennrich AA, Conzelmann KK, Gogolla N. A whole-brain connectivity map of mouse insular cortex. *Elife.* 9, 2020

19. Goldberg DS, McGee SJ. Pain as a global public health priority. *BMC Public Health.* 11:770, 2011

20. Gu X, Hof PR, Friston KJ, Fan J. Anterior insular cortex and emotional awareness. *J Comp Neurol.* 521:3371-3388, 2013

21. Gussew A, Rzanny R, Erdtel M, Scholle HC, Kaiser WA, Mentzel HJ, Reichenbach JR. Time-resolved functional 1H MR spectroscopic detection of glutamate concentration changes in the brain during acute heat pain stimulation. *Neuroimage.* 49:1895-1902, 2010

22. Gutzeit A, Meier D, Froehlich JM, Hergan K, Kos S, C VW, Lutz K, Ettlin D, Binkert CA, Mutschler J, Sartoretti-Schefer S, Brugger M. Differential NMR spectroscopy reactions of anterior/posterior and right/left insular subdivisions due to acute dental pain. *Eur Radiol.* 23:450-460, 2013

23. Harris RE, Sundgren PC, Craig AD, Kirshenbaum E, Sen A, Napadow V, Clauw DJ. Elevated insular glutamate in fibromyalgia is associated with experimental pain. *Arthritis Rheum.* 60:3146-3152, 2009

24. Jasmin L, Burkey AR, Granato A, Ohara PT. Rostral agranular insular cortex and pain areas of the central nervous system: a tract-tracing study in the rat. *J Comp Neurol.* 468:425-440, 2004

25. Jee Kim M, Tanioka M, Woo Um S, Hong SK, Hwan Lee B. Analgesic effects of FAAH inhibitor in the insular cortex of nerve-injured rats. *Mol Pain.* 14:1744806918814345, 2018

26. Ju A, Fernandez-Arroyo B, Wu Y, Jacky D, Beyeler A. Expression of serotonin 1A and 2A receptors in molecular- and projection-defined neurons of the mouse insular cortex. *Mol Brain.* 13:99, 2020

27. Khasar SG, Isenberg WM, Miao FJ, Gear RW, Green PG, Levine JD. Gender and gonadal hormone effects on vagal modulation of tonic nociception. *J Pain.* 2:91-100, 2001

28. Klarer M, Arnold M, Gunther L, Winter C, Langhans W, Meyer U. Gut vagal afferents differentially modulate innate anxiety and learned fear. *J Neurosci.* 34:7067-7076, 2014

29. Kobrzycka A, Napora P, Pearson BL, Pierzchala-Koziec K, Szewczyk R, Wieczorek M. Peripheral and central compensatory mechanisms for impaired vagus nerve function during peripheral immune activation. *J Neuroinflammation.* 16:150, 2019

30. Lee GJ, Kim SA, Kim YJ, Oh SB. Naloxone-induced analgesia mediated by central kappa opioid system in chronic inflammatory pain. *Brain Res.* 1762:147445, 2021

31. Lee GJ, Kim YJ, Lee K, Oh SB. Patterns of brain c-Fos expression in response to feeding behavior in acute and chronic inflammatory pain condition. *Neuroreport.* 32:1269-1277, 2021

32. Lee GJ, Kim YJ, Lee K, Oh SB. Patterns of brain c-Fos expression in

response to feeding behavior in acute and chronic inflammatory pain condition. *Neuroreport.* 2021

33. Lee JY, Lee GJ, Lee PR, Won CH, Kim D, Kang Y, Oh SB. The analgesic effect of refeeding on acute and chronic inflammatory pain. *Sci Rep.* 9:16873, 2019

34. Lee JY, Lee GJ, Nakamura A, Lee PR, Kim Y, Won CH, Furue H, Oh SB. Involvement of cannabinoid type 1 receptor in fasting-induced analgesia. *Mol Pain.* 16:1744806920969476, 2020

35. Levinthal DJ, Strick PL. Multiple areas of the cerebral cortex influence the stomach. *Proc Natl Acad Sci U S A.* 117:13078-13083, 2020

36. Liu XB, Murray KD. Neuronal excitability and calcium/calmodulin-dependent protein kinase type II: location, location, location. *Epilepsia.* 53 Suppl 1:45-52, 2012

37. Lu C, Yang T, Zhao H, Zhang M, Meng F, Fu H, Xie Y, Xu H. Insular Cortex is Critical for the Perception, Modulation, and Chronification of Pain. *Neurosci Bull.* 32:191-201, 2016

38. Mao J, Mayer DJ, Price DD. Patterns of increased brain activity indicative of pain in a rat model of peripheral mononeuropathy. *J Neurosci.* 13:2689-2702, 1993

39. Medeiros Pd: Envolvimento dos sistemas glutamatérgico, endocanabinoide e endovaniloide do córtex pré-frontal medial no modelo de dor neuropática e na comorbidade dor crônica e ansiedade/pânico, 2017.

40. Mordes JP, el Lozy M, Herrera MG, Silen W. Effects of vagotomy with and without pyloroplasty on weight and food intake in rats. *Am J Physiol.* 236:R61-66, 1979

41. Nahin RL. Estimates of pain prevalence and severity in adults: United States, 2012. *J Pain.* 16:769-780, 2015

42. Nogueira PJ, Tomaz C, Williams CL. Contribution of the vagus nerve in mediating the memory-facilitating effects of substance P. *Behav Brain Res.* 62:165-169, 1994

43. Oi M, Kobayashi K. Vagotomy as a surgical procedure for relief of pain. *Am J Surg.* 106:49-56, 1963

44. Ondicova K, Tillinger A, Pecenak J, Mravec B. The vagus nerve role in

antidepressants action: Efferent vagal pathways participate in peripheral anti-inflammatory effect of fluoxetine. *Neurochem Int.* 125:47-56, 2019

45. Ong WY, Stohler CS, Herr DR. Role of the Prefrontal Cortex in Pain Processing. *Mol Neurobiol.* 56:1137-1166, 2019

46. Park HJ, Moon DE. Pharmacologic management of chronic pain. *Korean J Pain.* 23:99-108, 2010

47. Peters JH, Gallaher ZR, Ryu V, Czaja K. Withdrawal and restoration of central vagal afferents within the dorsal vagal complex following subdiaphragmatic vagotomy. *J Comp Neurol.* 521:3584-3599, 2013

48. Pu Y, Tan Y, Qu Y, Chang L, Wang S, Wei Y, Wang X, Hashimoto K. A role of the subdiaphragmatic vagus nerve in depression-like phenotypes in mice after fecal microbiota transplantation from Chrna7 knock-out mice with depression-like phenotypes. *Brain Behav Immun.* 94:318-326, 2021

49. Qian K, Liu J, Cao Y, Yang J, Qiu S. Intraperitoneal injection of lithium chloride induces lateralized activation of the insular cortex in adult mice. *Mol Brain.* 14:71, 2021

50. Rothemeyer SJ, Enslin JMN. Surgical management of pain. *SAMJ: South African Medical Journal.* 106:858-860, 2016

51. Saleh TM, Connell BJ, Legge C, Cribb AE. Estrogen attenuates neuronal excitability in the insular cortex following middle cerebral artery occlusion. *Brain Res.* 1018:119-129, 2004

52. Savage S, Ma D. Experimental behaviour testing: pain. *Br J Anaesth.* 114:721-724, 2015

53. Spuz CA, Tomaszycki ML, Borszcz GS. N-methyl-D-aspartate receptor agonism and antagonism within the amygdaloid central nucleus suppresses pain affect: differential contribution of the ventrolateral periaqueductal gray. *J Pain.* 15:1305-1318, 2014

54. Takeda R, Watanabe Y, Ikeda T, Abe H, Ebihara K, Matsuo H, Nonaka H, Hashiguchi H, Nishimori T, Ishida Y. Analgesic effect of milnacipran is associated with c-Fos expression in the anterior cingulate cortex in the rat neuropathic pain model. *Neurosci Res.* 64:380-384, 2009

55. Tsurugizawa T, Uematsu A, Nakamura E, Hasumura M, Hirota M, Kondoh T, Uneyama H, Torii K. Mechanisms of neural response to gastrointestinal

nutritive stimuli: the gut-brain axis. *Gastroenterology.* 137:262-273, 2009

56. Wang X, Wu Q, Egan L, Gu X, Liu P, Gu H, Yang Y, Luo J, Wu Y, Gao Z, Fan J. Anterior insular cortex plays a critical role in interoceptive attention. *Elife.* 8, 2019

57. Watson CJ. Insular balance of glutamatergic and GABAergic signaling modulates pain processing. *Pain.* 157:2194-2207, 2016

58. Zhuo M. Contribution of synaptic plasticity in the insular cortex to chronic pain. *Neuroscience.* 338:220-229, 2016

59. Zurowski D, Nowak L, Wordliczek J, Dobrogowski J, Thor PJ. Effects of vagus nerve stimulation in visceral pain model. *Folia Med Cracov.* 52:57-69, 2012

.

국문초록

급성 통증에 대한 횡경막 아래 미주신경절단술의 효과

횡경막 아래 미주신경절단술 (Subdiaphragmatic vagotomy)은 내장 통증뿐만 아니라 말초 통증 등 다양한 통증 조건에서 진통 효과를 낸다. 포르말린 유도 급성 염증성 통증 모델을 이용해 횡경막 아래 미주신경절단술이 어떻게 말초 통증 상태에서 진통 효과를 유도하는 지를 규명하는 것을 목표로 했다. 뇌 전체의 신경 활성 지표 발현을 분석하고, 급성 염증성 통증 아래에서 횡경막 아래 미주신경절단술의 유도 진통 효과를 매개하는 특정 뇌 부위를 확인했다. 급성 염증성 통증에서 섬 피질의 하위 영역 중 전방 섬피질 (腦島葉, anterior insular cortex)에서 특히 신경 활성 지표 발현이 증가했으며, 이는 횡경막 아래 미주신경절단술에 의해 역전되었다. 이러한 결과는 암컷 생쥐에서 모방되지 않았으며, 이는 횡경막 아래 미주신경절단술로 유도되는 진통 효과의 성적 이형성을 나타낸다. 횡경막 아래 미주신경절단술은 전방 섬피질 (腦島葉)에서 가바성 뉴런보다 글루탐산성 뉴런에서 선호적으로 신경 활성 지표 발현이 감소되었으며, 전방 섬피질 (腦島葉)의 글루탐산성 뉴런을 NMDA(1 μg/μL)로 약리적 활성화를 일으켰을 때 횡경막 아래 미주신경절단술의 유도 진통 효과가 억제되었다. 종합하면, 이 연구는 전방 섬피질 (腦島葉)에서 글루탐산성 뉴런의 신경 활성 감소가 횡경막 아래 미주신경절단술의 유도 진통 효과를 매개하며 염증성 통증을 치료하는 중요한 치료 표적이 될 수 있음을 시사한다.

주요어: 횡경막 아래 미주신경절단술; 급성 염증성 통증; 전방 섬피질; 글루탐산성 신경

학번: 2020-27479